Research Article Vol. 11, No. 4 / April 2024 / Optica 485

Exceptional refrigeration of motions beyond their mass and temperature limitations

Deng-Gao Lai,[1,2,*] C.-H. Wang,[1] B.-P. Hou,[1] Adam Miranowicz,[2,3] and Franco Nori[2,4,5]

[1]College of Physics and Electronic Engineering, Institute of Solid Physics, Sichuan Normal University, Chengdu 610101, China
[2]Theoretical Quantum Physics Laboratory, Cluster for Pioneering Research, RIKEN, Wako shi, Saitama 351-0198, Japan
[3]Institute of Spintronics and Quantum Information, Faculty of Physics, Adam Mickiewicz University, 61-614 Poznań, Poland
[4]Center for Quantum Computing, RIKEN, Wako shi, Saitama 351-0198, Japan
[5]Physics Department, University of Michigan, Ann Arbor, Michigan 48109-1040, USA
*denggaolai@foxmail.com

Received 11 May 2023; revised 18 December 2023; accepted 7 January 2024; published 8 April 2024

Coaxing vibrations in the regimes of both large mass and high temperature into their motional quantum ground states is extremely challenging, because it requires an ultra-high optical power, which introduces extraneous excessive heating and intricate instabilities. Here we propose how to overcome these obstacles and cool vibrational networks by simply harnessing the power of an exceptional point (EP) induced in parity-time symmetric structures; and we reveal its exceptional cooling properties otherwise unachievable in conventional devices. In stark contrast to standard-cooling protocols, a three orders-of-magnitude amplification in net cooling rates arises from the EP-cooling mechanism, without which it vanishes. Remarkably, our EP cooling is nearly immune to both resonator mass and environmental temperature, and this overthrows the consensus that poor intrinsic factors and rugged extrinsic environment suppress cooling channels. Our study offers the possibility of isolating and engineering motional properties of large-mass and high-temperature objects for various applications in optical and acoustic sensing, gravimetry, and inertial navigation.

https://doi.org/10.1364/OPTICA.495199

1. INTRODUCTION

Quantum refrigeration of large-mass oscillators is an essential prerequisite for revealing genuine effects of quantum mechanics at large-mass scales, observing significant quantum signatures of mechanical motion, and probing quantum gravity on massive mechanical systems [1–15]. This is because thermal noise in these oscillators destroys quantum coherence signatures [1–3], precludes the exploration of macroscopic quantum phenomena [4–6], and limits the sensitivity of massive mechanical transducers in metrology and sensing applications [7–15].

Over the past few decades, significant developments have been accomplished in cooling the mechanical resonator to its motional quantum ground state, which has been widely reported both theoretically [16–19] and experimentally [20–27], using cavity optomechanical platforms [28–31]. However, these proposals and experiments still inherently suffer from both large-mass and high-temperature limitations [32–35], which are a major challenge for the preparation of such extremely fragile quantum ground states. The physical origin behind these obstacles is that a large optical power, which is required to cool a large-mass resonator, introduces extraneous excessive heating and intricate instabilities [30]. Especially, a high-temperature environment in the large-mass regime accelerates intrinsic thermal motion and blocks efficient light-motion refrigeration. Besides these issues, quantum ground-state refrigeration of vibrational networks in the large-mass and high-temperature regimes is ultimately required, in terms of the practical applicability of modern quantum technologies for quantum networks [36–45].

Here we propose a *simple* use of an exceptional point (EP) to overcome these cooling obstacles originating from both resonator-mass and environmental-temperature limitations, and to achieve an exceptional refrigeration of motional networks. We recall that EPs correspond to non-Hermitian spectral degeneracies featuring the simultaneous coalescence of both eigenstates and associated eigenvalues [46–55]. Quantum systems with EPs show a variety of counterintuitive phenomena and intriguing physical effects, e.g., chiral perfect absorption [56], exceptional single-photon sources [57,58], loss-induced lasing [59–61], and giant-enhanced sensing [62–67], which have no correspondence to their Hermitian counterparts.

We show that a giant enhancement can be achieved for optomechanical refrigeration of the large-mass motion at an EP, which is induced in parity-time ($\mathcal{PT}$) symmetric setups consisting of gain and loss cavities. Note that $\mathcal{PT}$-symmetry quantum devices exhibit an EP when switching the unbroken to broken $\mathcal{PT}$-symmetric regimes [46,47,68–82]. We reveal that the *contamination-tolerant* robustness against a high-temperature environment for the EP-cooling mechanism can be observed to be more than *three orders of magnitude* stronger than that in

the standard-cooling (i.e., resolved-sideband-cooling) protocols [16–18]. Physically, the application of EP technologies to optomechanical networks induces a strong field-localization effect [59,75–78], which dramatically amplifies the net-refrigeration rate of the vibration. Specifically, the excitations concentrate in the active cavity leading to a faster depletion of the excitations in the original passive cavity and thus to an enhanced cooling rate for the vibration. Note that our EP refrigeration is an *intensive* cooling based on the sideband-cooling technique, and this occurs because of the synergy of the field-localization effect and the sideband-cooling mechanism.

Optomechanical refrigeration in the standard-cooling schemes becomes much worse with increasing resonator mass [16–24,83], while, surprisingly, in our EP cooling, it is nearly *independent* of the mass. Physically, the refrigeration rate significantly reduces, due to the decrease of the light-motion coupling strength with increasing resonator mass, while it can be completely compensated for or even greatly amplified by employing the field-localization effect [59,75–78]. These results indicate that our proposed ultrahigh-efficiency optomechanical cooling, with *immunity* against both environmental noise and resonator mass, can be realized by simply utilizing an EP, without the need of any high-cost and colossal LIGO gravitational-wave detectors [84] or magnomechanical materials [85]. In a broader view, our study sheds new light on the synergy of optomechanical-network and EP technologies, and offers exciting opportunities of cooling large-mass and high-temperature quantum devices to their motional quantum ground states. *This is usually impossible with standard-cooling protocols* [16–31,86–92], while our method can lead to a wide range of applications, e.g., both mass-immune and noise-tolerant quantum sensing, quantum processing, and quantum networks.

2. RESULTS

A. System and Its Exceptional Point

We consider an EP-assisted optomechanical network, where N vibrations are optomechanically coupled to a passive cavity, linked to an active cavity [see Fig. 1(a)]. An EP supported in the loss-gain optical system occurs via the transition from the $\mathcal{PT}$-symmetric to symmetry-broken regimes. A driving laser (with amplitude $|\varepsilon_L| = \sqrt{2\kappa_c P_L/\hbar\omega_L}$, frequency ω_L, and laser power P_L) is applied to the loss cavity. In a rotating frame, defined by the unitary transformation operator $\exp[-i\omega_L(c^\dagger c + a^\dagger a)t]$, the Hamiltonian reads ($\hbar = 1$)

$$\mathcal{H}_I = \Delta_c c^\dagger c + \Delta_a a^\dagger a + \sum_{j=1}^{N}\left[\omega_j b_j^\dagger b_j + g_j c^\dagger c\left(b_j^\dagger + b_j\right)\right] + J\left(c^\dagger a + c a^\dagger\right) + i\varepsilon_L\left(c^\dagger - c\right), \tag{1}$$

where $a^\dagger$ (a), $c^\dagger$ (c), and $b_j^\dagger$ (b_j) are, respectively, the creation (annihilation) operators of the gain cavity (with resonance frequency ω_a), the loss cavity (with resonance frequency ω_c), and the jth vibration with resonance frequency ω_j and initial mean thermal excitation number $\bar{n}_{\mathrm{th},j} = \{\exp[\hbar\omega_j/(k_B T_j)] - 1\}^{-1}$, where T_j is the bath temperature, which can be different for different modes; hence T_j has a subscript. The light-vibration interactions between the loss optical mode c and the jth vibrational mode are described by the g_j terms, where $g_j = (\omega_c/L)\sqrt{\hbar/(2m_j\omega_j)}$, with the resonator mass m_j and cavity length L. We see from the expression of g_j that for a large-mass mechanical resonator, the decrease in the zero-point motion [i.e., $\sqrt{\hbar/(2m_j\omega_j)}$] with the mass leads to a greatly reduced light-motion coupling strength, making its ground-state cooling hard to achieve. The J term is the photon-tunneling interaction between the two optical modes. The ε_L term describes the cavity-field driving, with $\Delta_{c(a)} = \omega_{c(a)} - \omega_L$ representing the driving detuning for the loss (gain) cavity.

To demonstrate the EP of the system, first we only consider a coupled passive-active optical construction, and then its effective Hamiltonian, taking both dissipation (κ_c) and gain (κ_a) rates into consideration, can be expressed as

$$\mathcal{H}_{\mathrm{coupl}} = \omega_c c^\dagger c + \omega_a a^\dagger a - i\kappa_c c^\dagger c + i\kappa_a a^\dagger a + J(c^\dagger a + c a^\dagger). \tag{2}$$

By considering two degenerate optical modes, $\omega_c = \omega_a \equiv \omega_0$, and introducing two supermodes, $\mathcal{A}_\pm = (c \pm a)/\sqrt{2}$, we obtain $\mathcal{H}_{\mathrm{coupl}} = \sum_\pm \omega_\pm \mathcal{A}_\pm^\dagger \mathcal{A}_\pm$, where the corresponding complex eigenvalues are $\omega_\pm = \omega_0 - i\chi_- \pm \sqrt{J^2 - \chi_+^2}$, with $\chi_\pm = (\kappa_c \pm \kappa_a)/2$. The real and imaginary parts of $\omega_\pm$ are, respectively, the eigenfrequencies and the linewidths. The system is $\mathcal{PT}$-symmetric when this Hamiltonian remains unchanged under both parity- and time-reversal transformations, and it indicates that a phase

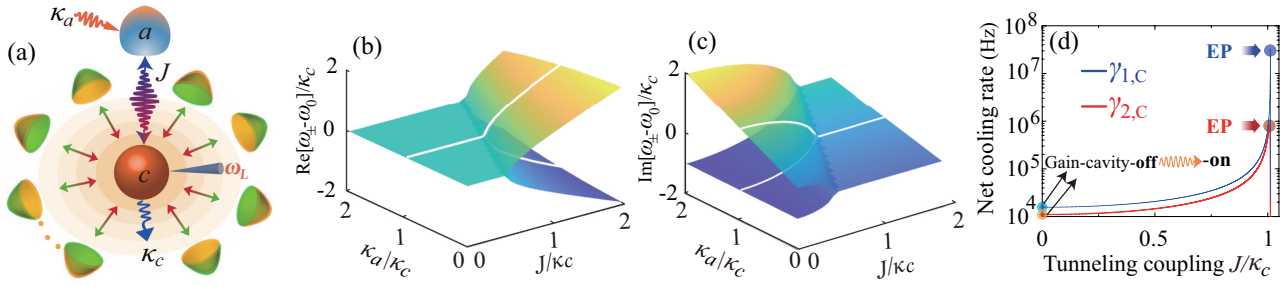

Fig. 1. (a) EP-assisted optomechanical networks, where a passive optical mode c (with decay rate κ_c and driving-laser frequency ω_L) is both coupled to an active optical mode a (with gain rate κ_a) via a photon-tunneling interaction J, and coupled to N vibrational modes $b_{j\in[1,N]}$ (with mechanical damping rate γ_j) by optomechanical-coupling rates g_j. (b) Real $\mathrm{Re}[\omega_\pm - \omega_0]/\kappa_c$ and (c) imaginary $\mathrm{Im}[\omega_\pm - \omega_0]/\kappa_c$ parts of the eigenfrequencies versus J/κ_c and κ_a/κ_c reveal spectral properties of the $\mathcal{PT}$ symmetry, when $\omega_c = \omega_a \equiv \omega_0$. The white solid curves depict the case when gain and loss are balanced: $\kappa_a = \kappa_c$. (d) Net cooling rate $\gamma_{j,C}$ versus J when $\kappa_a = \kappa_c$. Note that in (d), the two-peak points denote the maximal net cooling rates at the EP (i.e., $J/\kappa_c \approx 1$), and the term "Gain-cavity-off (on)" refers to the case when the gain cavity is turned off (on), i.e., $J/\kappa_c = 0$ ($J/\kappa_c \neq 0$). (b)–(d) correspond to the two-motional-mode case ($N = 2$). Other parameters are: $\omega_1/(2\pi) = 20$ MHz, $\omega_2/\omega_1 = 0.7$, $\gamma_j/\omega_1 = 10^{-5}$, $m_j = 100$ ng, $\kappa_c/\omega_1 = 1/(5\pi)$, $G_j/\kappa_c = 0.05$, and $\omega/\omega_1 = 0.99$ (corresponding to an optimal cooling rate [93]).

transition (i.e., at an EP) occurs from the $\mathcal{PT}$-symmetric to broken-$\mathcal{PT}$-symmetric regimes [46,47,68–82].

Specifically, we see from Figs. 1(b) and 1(c) that when $J > \kappa_c$ ($J < \kappa_c$), the eigenfrequencies have an identical imaginary (real) part and two different real (imaginary) parts. This indicates that the system possesses the $\mathcal{PT}$ (broken-$\mathcal{PT}$) symmetry with an identical linewidth (frequency) and two different frequencies (linewidths). In particular, the EP (e.g., at $J \approx \kappa_c$ when $\kappa_a = \kappa_c$; see white solid curves), where the eigenstates coalesce, emerges due to the switching between the broken and unbroken $\mathcal{PT}$-symmetric regimes. At this EP, a more than *three-orders-of-magnitude* amplification of the net cooling rate can be achieved, which is otherwise *unattainable* in conventional optomechanical devices, as shown in Fig. 1(d). Physically, the phonons concentrate in the gain cavity leading to a faster depletion of the phonons in the loss cavity and thus to an enhanced refrigeration rate for the vibration. In our numerical simulations, the maximum achievable cooling rate can be observed when J is very close to (but slightly smaller than) κ_c. During an experiment, if the value of J/κ_c fluctuates, it could be possible to push the system from experiencing strong cooling ($J < \kappa_c$) to cooling suppression ($J > \kappa_c$) [93]. This would constitute a limiting instability for realizable cooling.

B. Numerical and Analytical Results

By applying a strong optical driving, the dynamics of the system can be linearized by expanding all the operators as sums of their steady-state mean values and quantum fluctuations, i.e., $a(c) = \alpha_{1(2)} + \delta a(c)$ and $b_j = \beta_j + \delta b_j$. After ignoring higher-order terms of quantum fluctuations, we obtain the linearized equations of motion for quantum fluctuations: $\dot{\boldsymbol{u}}(t) = \mathbf{A}\mathbf{u}(t) + \mathbf{N}(t)$, where we introduce the fluctuation operator vector $\mathbf{u}(t) = (\delta c, \delta c^\dagger, \delta a, \delta a^\dagger, \delta b_1, \delta b_1^\dagger, \ldots, \delta b_N, \delta b_N^\dagger)^T$, the noise operator vector $\mathbf{N}(t) = \sqrt{2}(\sqrt{\kappa_c}c_{\rm in}, \sqrt{\kappa_c}c_{\rm in}^\dagger, \sqrt{\kappa_a}a_{\rm in}, \sqrt{\kappa_a}a_{\rm in}^\dagger, \sqrt{\gamma_1}b_{1,\rm in}, \sqrt{\gamma_1}b_{1,\rm in}^\dagger, \ldots, \sqrt{\gamma_N}b_{N,\rm in}, \sqrt{\gamma_N}b_{N,\rm in}^\dagger)^T$, and the coefficient matrix $\mathbf{A}$ given in [93], with the effective driving detuning for the loss (gain) cavity $\Delta_1 = \Delta_c + \sum_{j=1}^N g_j(\beta_j^* + \beta_j)$ ($\Delta_2 = \Delta_a$), and the effective optomechanical-coupling strength $G_j = g_j\alpha_2$ for the jth vibrational mode [93]. Without loss of generality, hereafter, we assume $\Delta \equiv \Delta_1 \approx \Delta_2$. All the parameters satisfy the stability conditions derived from the Routh-Hurwitz criterion [94].

The *numerical* results of the steady-state mean phonon numbers in these vibrations can be obtained via the Lyapunov equation $\mathbf{A}\mathbf{V} + \mathbf{V}\mathbf{A}^T = -\mathbf{Q}$, where the covariance matrix $\mathbf{V}$ is defined by the matrix elements $\mathbf{V}_{ij} = [\langle \mathbf{u}_i(\infty)\mathbf{u}_j(\infty)\rangle + \langle \mathbf{u}_j(\infty)\mathbf{u}_i(\infty)\rangle]/2$, for $i, j = 1, \ldots, (2N+4)$, and the matrix $\mathbf{Q} = (\mathbf{C} + \mathbf{C}^T)/2$, with the noise correlation matrix $\mathbf{C}$ defined by the matrix elements $\langle \mathbf{N}_k(s)\mathbf{N}_l(s')\rangle = \mathbf{C}_{k,l}\delta(s - s')$. Then we derive the final mean phonon numbers of the jth vibration [93]:

$$n_{j\in[1,N]}^{f,\rm Num} = \mathbf{V}_{(2j+4)(2j+3)} - 1/2, \tag{3}$$

where $\mathbf{V}_{(2j+4)(2j+3)}$ is obtained from the Lyapunov equation. By introducing the position and momentum operators $x_j = \sqrt{\hbar/(2m_j\omega_j)}(b_j^\dagger + b_j)$ and $p_{x_j} = i\sqrt{m_j\hbar\omega_j/2}(b_j^\dagger - b_j)$, the *analytical* results of the final average thermal occupation numbers can be calculated by the relation [93]

$$n_{j\in[1,N]}^{f,\rm Anal} = \left[\langle \delta q_j^2\rangle + \langle \delta p_j^2\rangle - 1\right]/2, \tag{4}$$

where $\langle \delta q_j^2\rangle = (1/2\pi)\int_{-\infty}^{\infty} S_{q_j}(\omega)\mathrm{d}\omega$ and $\langle \delta p_j^2\rangle = (1/2\pi)\int_{-\infty}^{\infty} S_{p_j}(\omega)\mathrm{d}\omega$, with the fluctuation spectra $S_{o=q_j,p_j}(\omega) = \int_{-\infty}^{\infty}\exp(-i\omega\tau)\langle \delta o(t+\tau)\delta o(t)\rangle_{\rm ss}\mathrm{d}\tau$ (see Supplement 1 for more analytical details [93–95]).

The analytical *net* refrigeration rate of the jth motional mode, when considering the case of $N = 2$ and $\kappa_{c(a)} = \kappa_0$, is derived as

$$\gamma_{j,C} = 4G_j^2\left[1 + \chi_j(J, \Delta)\right]/\kappa_0, \tag{5}$$

where $\chi_j(J, \Delta)$ is the cooling-enhancement factor induced by the EP effect, given in [93].

C. EP Cooling Immune to Both Temperature and Mass

To demonstrate the exceptional refrigeration of this complex system, we first consider the case of $N = 2$. In Figs. 2(a) and 2(b), the net cooling rate $\gamma_{j,C}$ is plotted versus the effective driving detuning Δ, when the system operates in both standard cooling (blue curves) and EP cooling (red curves). It shows that the maximum net cooling rate emerges around the red-sideband resonance ($\Delta \approx \omega_1$), and especially, the net refrigeration rate in the EP-cooling case can be *three orders of magnitude* larger than that for the standard cooling. Physically, the strong field-localization effect [59,75–78] induced by our EP system dramatically enhances the generation rate of the anti-Stokes photons; and meanwhile it extremely reduces the excitation-exchange rate in the swap-heating processes. These results indicate that, in general, by simply employing an EP, the cooling rate of the vibration can be greatly amplified and engineered.

In our system, a passive optical mode, connected to an active optical mode, is simultaneously coupled to multiple vibrational modes (yielding in-parallel optomechanical interactions), each of which is not coupled to each other. For convenience, we here explain the physical mechanism of the EP cooling for the jth vibrational mode. Physically, the thermal phonons stored in the vibrational mode are first extracted into the loss cavity and then these thermal excitations flow into the gain cavity and finally localize there, which results in energy localization [59,75–78]. In this case, the cooling rate of the motional mode can be greatly amplified by the energy localization in the active cavity a. Specifically, we can see from Fig. 2(e) [78] that the absorption rate of anti-Stokes photons [corresponding to the field-localization-cooling process] of the passive cavity c can be dramatically enhanced, compared with the standard resolved-sideband optomechanical cooling for which there is only cavity dissipation [i.e., the DC process]. Meanwhile, the heat-exchange rate [i.e., the SH process] is greatly reduced, owing to the joint effect of the field localization and the decrease of anti-Stokes photons [77,78]. These findings indicate that the field-localization effect can enable a dynamical enhancement in the refrigeration rate of the mechanical vibration. Our results on the EP cooling differ from what is known in the literatures [77,78], mainly because we are interested not in a single mechanical motion but in the vibrational networks.

To further elucidate this EP-intensive cooling, we plot in Figs. 2(c) and 2(d) the final mean phonon numbers n_j^f versus the environmental temperature T_j for both standard cooling (blue curves) and EP cooling (red curves). It is clearly shown that, with increasing T_j, the motional degree of freedom in the EP-cooling case can be effectively cooled and its cooling performance can be improved up to *three* orders of magnitude compared with the

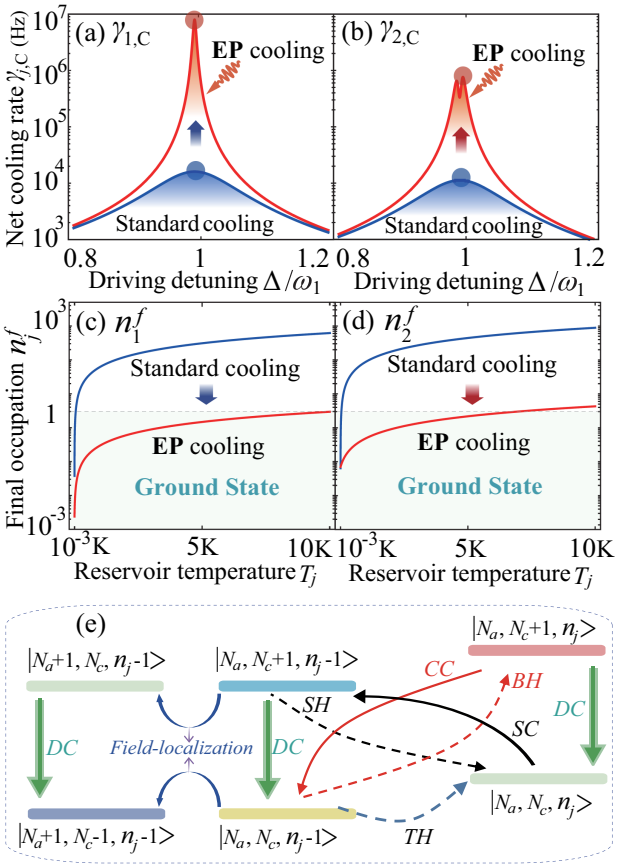

Fig. 2. Net cooling rates (a) $\gamma_{1,C}$ and (b) $\gamma_{2,C}$ versus the effective driving detuning Δ in both standard cooling (blue curves, $J/\kappa_c = 0$) and EP cooling (red curves, $J/\kappa_c = 0.999$). Final mean occupation numbers (c) n_1^f and (d) n_2^f versus the reservoir temperature T_j when $\Delta = \omega_j$. Other parameters are the same as those in Fig. 1. (e) Energy-level diagram of the EP-cooling mechanism [78]. The number state is described by $|N_a, N_c, n_j\rangle$, with N_a (N_c) being the photon number of the gain (loss) optical mode, and n_j denoting the thermal phonon number of the jth vibrational mode. The dashed curves depict the heating processes: back-action heating (BH), swap heating (SH), and thermal heating (TH). The solid curves denote the refrigeration processes: swap cooling (SC), counter-wave cooling (CC), dissipation cooling (DC) by the loss-optical mode c, and the field-localization cooling by the gain-optical mode a.

standard-cooling performance. Remarkably, the threshold reservoir temperature for preserving quantum ground-state cooling in the EP cooling, is nearly *three* orders of magnitude higher than that in the standard cooling. The underlying physical mechanism behind this counterintuitive phenomenon can be explained as follows: the introduced EP leads to a giant enhancement of the net cooling rate, and this breaks the law that the cooling rate is commonly suppressed by the rugged high-temperature environment. These results provide the means to protect fragile quantum mechanical setups from environmental thermal noises, and pave a way towards *noise-tolerant* quantum vibrational networks.

To show the *immunity* of the EP-cooling mechanism against resonator mass, we make a detailed comparison between the standard- and EP-cooling performances versus the mass, using both numerical (curves) and analytical (symbols) results, as shown in Figs. 3(a) and 3(b). Clearly, the numerical and analytical predictions match well with each other. The EP-cooling technique allows us to reach the motional quantum ground state in the large-mass

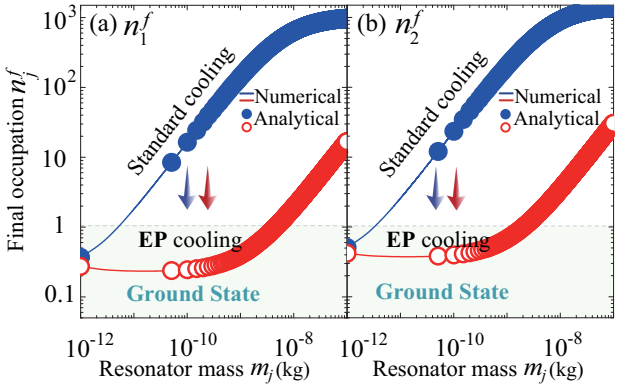

Fig. 3. Final average thermal occupation numbers (a) n_1^f and (b) n_2^f versus the resonator mass m_j in both standard cooling (blue curves and symbols, $J/\kappa_c = 0$) and EP cooling (red curves and symbols, $J/\kappa_c = 0.999$). The curves show the numerical predictions [see Eq. (3)], while the symbols correspond to analytical results [see Eq. (4)]. Clearly, an excellent agreement between the numerical and analytical results is seen. Note that the masses of the two oscillators are in general different; however, for convenience, we consider the case where both masses are equal in our simulations. Here $T_j = 1$ K, $\omega_c/(2\pi) = 2.817 \times 10^{14}$ Hz, $L = 1$ mm, $\lambda = 1064$ nm, $P_L = 9$ mW, and other parameters are the same as those in Fig. 1.

regime, which is very challenging for the standard-cooling schemes [16–31,86–92]. We also reveal that near the EP, the maximum refrigeration rate is insensitive to the resonator mass. Specifically, in the EP-cooling case, the threshold mass for preserving quantum ground-state cooling has been predicted to be more than three orders of magnitude larger than that in the standard-cooling case. Physically, the net cooling rate is reduced due to the decrease in the light-motion coupling strength with increasing the resonator mass, while it can be tremendously compensated for or even amplified by employing the EP-cooling mechanism. Our findings mean that the EP-cooling mechanism paves a route towards exploiting quantum ground-state preparation *immune* to the device mass.

D. Cooling *N*-vibration Optomechanical Networks

The EP-cooling mechanism can be generalized to the exceptional refrigeration of N-vibration optomechanical networks, which are coupled to a common passive cavity-field mode, as shown in Fig. 1(a). We see from Fig. 4 that quantum ground-state cooling of the motion *cannot* be achieved (see green rectangles) in the standard cooling. However, in stark contrast to this, it becomes *feasible* (see lower red disks) in the EP cooling. Physically, the introduced EP leads to amplifying the net cooling rate of the vibration, and produces a giant enhancement for the refrigeration performance. These results not only open the possibility of further largely suppressing thermal noise in vibrational networks, but also pave a route towards the preparation of nonclassical states of the motion, e.g., large spatial superpositions or non-Gaussian states (e.g., Schrödinger-cat-like states).

3. DISCUSSION AND CONCLUSIONS

In contrast to the previously established demonstrations investigating the exceptional cooling in single-vibration optomechanical platforms [77,78], we here focus on the EP-intensive cooling

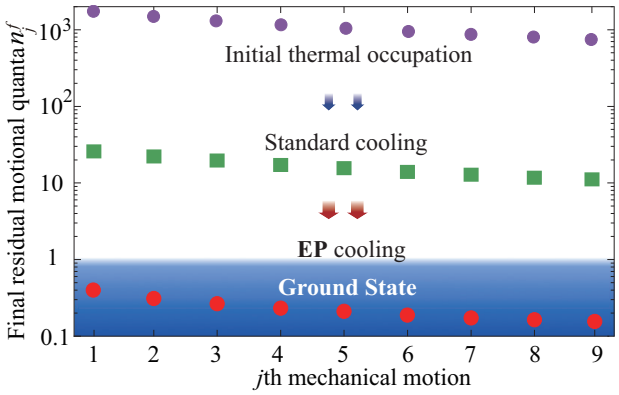

Fig. 4. Residual motional quanta numbers $n^f_{j\in[1,N]}$ versus the jth motion. The horizontal axis denotes the frequency dispersion relation of the vibrations with nine independent vibrational frequencies $(\omega_{1,\cdots,9})/\omega_m = 0.6, \ldots, 1.4$. The purple disks are the initial thermal occupations, while the green rectangles and red disks denote the final mean phonon numbers in the standard- and EP-cooling cases, respectively. Here $T_j = 1$ K, $G_j/\kappa_c = 0.1$, and other parameters are the same as those in Fig. 1.

using multi-vibration optomechanical networks [36–45] showing much richer and more general properties. In particular, our intrinsic motivations are not limited to studying the exceptional refrigeration of the vibration networks by both fully analytical and numerical treatments, but also to overcome a long-standing challenge that quantum ground-state cooling of the motion in the regimes of both large mass and high temperature is hard to achieve. This means that unlike the previous schemes [77,78], where the aim is to cool and isolate a single motion, the aim here is not only to quickly and exceptionally extract thermal phonons from vibrational networks but also to completely overcome the serious cooling obstacles originating from the resonator-mass and environmental-temperature limitations. Our study shows that by simply harnessing the power of an EP, one can achieve an ultra-high-efficiency cooling, which is immune to both resonator mass and environmental noise, without the need of using any high-cost low-loss materials and noise filters [96,97]. These cooling performances are otherwise unachievable in the previous studies [77,78].

In conclusion, we proposed a simple EP-cooling mechanism to amplify the net cooling rate of the vibration, and to effectively cool the motional degree of freedom down to the quantum ground state. We showed that the final mean thermal occupation numbers in the EP-cooling case are three orders of magnitude smaller than those for the standard cooling. In particular, we revealed that in the standard-cooling case, optomechanical cooling becomes much worse with increasing either environmental temperature or resonator mass, while in the EP-cooling case, it is almost independent of these parameters. This study enables the exploration of quantum physics in large-mass and high-temperature quantum mechanical systems, and paves a way towards realizing pure quantum cavity optomechanics, with immunity against both resonator mass and environmental noise.

Funding. Japan Society for the Promotion of Science (P23027, JP20H00134); Sichuan Province Science and Technology Support Program (2018JY0180, 2021-YF05-02416-GX); National Natural Science Foundation of China (10647007, 11974009); Narodowe Centrum Nauki (DEC-2019/34/A/ST2/00081); Nippon Telegraph and Telephone Corporation (NTT) Research, the Japan Science and Technology Agency (JST) [via the Quantum Leap Flagship Program (Q-LEAP), and the Moonshot Research and Development Program (JPMJMS2061)]; Office of Naval Research (ONR) (N62909-23-1-2074).

Disclosures. The authors declare no conflicts of interest.

Data availability. Data underlying the results presented in this paper are not publicly available at this time but may be obtained from the authors upon reasonable request.

Supplemental document. See Supplement 1 for supporting content.

REFERENCES AND NOTES

1. F. Karolyhazy, "Gravitation and quantum mechanics of macroscopic objects," Nuovo Cim. A **42**, 390–402 (1966).
2. L. Diósi, "Models for universal reduction of macroscopic quantum fluctuations," Phys. Rev. A **40**, 1165–1174 (1989).
3. R. Penrose, "On gravity's role in quantum state reduction," Gen. Relativ. Gravit. **28**, 581–600 (1996).
4. O. Romero-Isart, A. C. Pflanzer, F. Blaser, *et al.*, "Large quantum superpositions and interference of massive nanometer sized objects," Phys. Rev. Lett. **107**, 020405 (2011).
5. A. T. M. A. Rahman, "Large spatial Schrödinger cat state using a levitated ferrimagnetic nanoparticle," New J. Phys. **21**, 113011 (2019).
6. P. Sekatski, M. Aspelmeyer, and N. Sangouard, "Macroscopic optomechanics from displaced single-photon entanglement," Phys. Rev. Lett. **112**, 080502 (2014).
7. B. P. Abbott, R. Abbott, T. D. Abbott, *et al.*, "The advanced LIGO detectors in the era of first discoveries," Phys. Rev. Lett. **116**, 131103 (2016).
8. J. Prat-Camps, C. Teo, C. C. Rusconi, *et al.*, "Ultrasensitive inertial and force sensors with diamagnetically levitated magnets," Phys. Rev. Appl. **8**, 034002 (2017).
9. F. Monteiro, G. Afek, D. Carney, *et al.*, "Search for composite dark matter with optically levitated sensors," Phys. Rev. Lett. **125**, 181102 (2020).
10. A. Bassi, A. Großardt, and H. Ulbricht, "Gravitational decoherence," Classical Quantum Gravity **34**, 193002 (2017).
11. M. P. Blencowe, "Effective field theory approach to gravitationally induced decoherence," Phys. Rev. Lett. **111**, 021302 (2013).
12. P. R. Saulson, "Thermal noise in mechanical experiments," Phys. Rev. D **42**, 2437–2445 (1990).
13. J. Millen and B. A. Stickler, "Quantum experiments with microscale particles," Contemp. Phys. **61**, 155–168 (2020).
14. M. Rademacher, J. Millen, and Y. L. Li, "Quantum sensing with nanoparticles for gravimetry: when bigger is better," Adv. Opt. Technol. **9**, 227–239 (2020).
15. D.-G. Lai, J.-Q. Liao, A. Miranowicz, *et al.*, "Noise-tolerant optomechanical entanglement via synthetic magnetism," Phys. Rev. Lett. **129**, 063602 (2022).
16. I. Wilson-Rae, N. Nooshi, W. Zwerger, *et al.*, "Theory of ground state cooling of a mechanical oscillator using dynamical backaction," Phys. Rev. Lett. **99**, 093901 (2007).
17. F. Marquardt, J. P. Chen, A. A. Clerk, *et al.*, "Quantum theory of cavity-assisted sideband cooling of mechanical motion," Phys. Rev. Lett. **99**, 093902 (2007).
18. C. Genes, D. Vitali, P. Tombesi, *et al.*, "Ground-state cooling of a micromechanical oscillator: comparing cold damping and cavity-assisted cooling schemes," Phys. Rev. A **77**, 033804 (2008).
19. C. Sommer and C. Genes, "Partial optomechanical refrigeration via multimode cold-damping feedback," Phys. Rev. Lett. **123**, 203605 (2019).
20. J. Chan, T. P. Alegre, A. H. Safavi-Naeini, *et al.*, "Laser cooling of a nanomechanical oscillator into its quantum ground state," Nature **478**, 89–92 (2011).
21. J. D. Teufel, T. Donner, D. Li, *et al.*, "Sideband cooling of micromechanical motion to the quantum ground state," Nature **475**, 359–363 (2011).
22. D. J. Wilson, V. Sudhir, N. Piro, *et al.*, "Measurement-based control of a mechanical oscillator at its thermal decoherence rate," Nature **524**, 325–329 (2015).
23. J. B. Clark, F. Lecocq, R. W. Simmonds, *et al.*, "Sideband cooling beyond the quantum limit with squeezed light," Nature **541**, 191–195 (2016).
24. U. Delić, M. Reisenbauer, K. Dare, *et al.*, "Cooling of a levitated nanoparticle to the motional quantum ground state," Science **367**, 892–895 (2020).
25. M. Rossi, N. Kralj, S. Zippilli, *et al.*, "Enhancing sideband cooling by feedback-controlled light," Phys. Rev. Lett. **119**, 123603 (2017).

26. M. Rossi, N. Kralj, S. Zippilli, *et al.*, "Normal-mode splitting in a weakly coupled optomechanical system," Phys. Rev. Lett. **120**, 073601 (2018).
27. M. Rossi, D. Mason, J. Chen, *et al.*, "Measurement-based quantum control of mechanical motion," Nature **563**, 53–58 (2018).
28. T. J. Kippenberg and K. J. Vahala, "Cavity optomechanics: back-action at the mesoscale," Science **321**, 1172–1176 (2008).
29. P. Meystre, "A short walk through quantum optomechanics," Ann. Phys. **525**, 215 (2013).
30. M. Aspelmeyer, T. J. Kippenberg, and F. Marquardt, "Cavity optomechanics," Rev. Mod. Phys. **86**, 1391–1452 (2014).
31. W. P. Bowen and G. J. Milburn, *Quantum Optomechanics* (CRC Press, 2015).
32. A. Ashkin and J. M. Dziedzic, "Optical levitation by radiation pressure," Appl. Phys. Lett. **19**, 283–285 (1971).
33. F. Monteiro, W. Li, G. Afek, *et al.*, "Force and acceleration sensing with optically levitated nanogram masses at microkelvin temperatures," Phys. Rev. A **101**, 053835 (2020).
34. G. Guccione, M. Hosseini, S. Adlong, *et al.*, "Scattering-free optical levitation of a cavity mirror," Phys. Rev. Lett. **111**, 183001 (2013).
35. Y. Michimura, Y. Kuwahara, T. Ushiba, *et al.*, "Optical levitation of a mirror for reaching the standard quantum limit," Opt. Express **25**, 13799–13806 (2017).
36. R. Riedinger, A. Wallucks, I. Marinković, *et al.*, "Remote quantum entanglement between two micromechanical oscillators," Nature **556**, 473–477 (2018).
37. C. F. Ockeloen-Korppi, E. Damskägg, J.-M. Pirkkalainen, *et al.*, "Stabilized entanglement of massive mechanical oscillators," Nature **556**, 478–482 (2018).
38. L. M. de Lépinay, C. F. Ockeloen-Korppi, M. J. Woolley, *et al.*, "Quantum mechanics-free subsystem with mechanical oscillators," Science **372**, 625–629 (2021).
39. S. Kotler, G. A. Peterson, E. Shojaee, *et al.*, "Direct observation of deterministic macroscopic entanglement," Science **372**, 622–625 (2021).
40. S. Armstrong, J.-F. Morizur, J. Janousek, *et al.*, "Programmable multimode quantum networks," Nat. Commun. **3**, 1026 (2012).
41. W. McCutcheon, A. Pappa, B. A. Bell, *et al.*, "Experimental verification of multipartite entanglement in quantum networks," Nat. Commun. **7**, 13251 (2016).
42. Y. Cai, J. Roslund, G. Ferrini, *et al.*, "Multimode entanglement in reconfigurable graph states using optical frequency combs," Nat. Commun. **8**, 15645 (2017).
43. S. Wengerowsky, S. K. Joshi, F. Steinlechner, *et al.*, "An entanglement-based wavelength-multiplexed quantum communication network," Nature **564**, 225–228 (2018).
44. J. P. Mathew, J. del Pino, and E. Verhagen, "Synthetic gauge fields for phonon transport in a nano-optomechanical system," Nat. Nanotechnol. **15**, 198–202 (2020).
45. J. del Pino, J. J. Slim, and E. Verhagen, "Non-Hermitian chiral phononics through optomechanically induced squeezing," Nature **606**, 82–87 (2022).
46. C. M. Bender and S. Boettcher, "Real spectra in non-Hermitian Hamiltonians having PT symmetry," Phys. Rev. Lett. **80**, 5243–5246 (1998).
47. C. M. Bender, "Making sense of non-Hermitian Hamiltonians," Rep. Prog. Phys. **70**, 947–1018 (2007).
48. Ş. K. Özdemir, S. Rotter, F. Nori, *et al.*, "Parity-time symmetry and exceptional points in photonics," Nat. Mater. **18**, 783–798 (2019).
49. R. El-Ganainy, M. Khajavikhan, D. N. Christodoulides, *et al.*, "The dawn of non-Hermitian optics," Commun. Phys. **2**, 37 (2019).
50. F. Minganti, A. Miranowicz, R. Chhajlany, *et al.*, "Quantum exceptional points of non-Hermitian Hamiltonians and Liouvillians: the effects of quantum jumps," Phys. Rev. A **100**, 062131 (2019).
51. F. Minganti, A. Miranowicz, R. W. Chhajlany, *et al.*, "Hybrid-Liouvillian formalism connecting exceptional points of non-Hermitian Hamiltonians and Liouvillians via postselection of quantum trajectories," Phys. Rev. A **101**, 062112 (2020).
52. E. J. Bergholtz, J. C. Budich, and F. K. Kunst, "Exceptional topology of non-Hermitian systems," Rev. Mod. Phys. **93**, 015005 (2021).
53. J. Peřma, A. Miranowicz, G. Chimczak, *et al.*, "Quantum Liouvillian exceptional and diabolical points for bosonic fields with quadratic Hamiltonians: the Heisenberg-Langevin equation approach," Quantum **6**, 883 (2022).
54. Z. Gong, Y. Ashida, K. Kawabata, *et al.*, "Topological phases of non-Hermitian systems," Phys. Rev. X **8**, 031079 (2018).
55. N. Wu, K. Cui, Q. Xu, *et al.*, "On-chip mechanical exceptional points based on an optomechanical zipper cavity," Sci. Adv. **9**, eabp8892 (2023).
56. S. Soleymani, Q. Zhong, M. Mokim, *et al.*, "Chiral and degenerate perfect absorption on exceptional surfaces," Nat. Commun. **13**, 599 (2022).
57. R. Huang, Ş. K. Özdemir, J.-Q. Liao, *et al.*, "Exceptional photon blockade: engineering photon blockade with chiral exceptional points," Laser Photon. Rev. **16**, 2100430 (2022).
58. Y. Zuo, R. Huang, L.-M. Kuang, *et al.*, "Loss-induced suppression, revival, and switch of photon blockade," Phys. Rev. A **106**, 043715 (2022).
59. B. Peng, Ş. K. Özdemir, S. Rotter, *et al.*, "Loss-induced suppression and revival of lasing," Science **346**, 328–332 (2014).
60. L. Feng, Z. J. Wong, R.-M. Ma, *et al.*, "Single mode laser by parity-time symmetry breaking," Science **346**, 972–975 (2014).
61. H. Hodaei, M.-A. Miri, M. Heinrich, *et al.*, "Parity-time-symmetric microring lasers," Science **346**, 975–978 (2014).
62. W. Chen, Ş. K. Özdemir, G. Zhao, *et al.*, "Exceptional points enhance sensing in an optical microcavity," Nature **548**, 192–196 (2017).
63. Z. Dong, Z. Li, F. Yang, *et al.*, "Sensitive readout of implantable microsensors using a wireless system locked to an exceptional point," Nat. Electron. **2**, 335–342 (2019).
64. Q. Zhong, J. Ren, M. Khajavikhan, *et al.*, "Sensing with exceptional surfaces in order to combine sensitivity with robustness," Phys. Rev. Lett. **122**, 153902 (2019).
65. Y.-H. Lai, Y.-K. Lu, M.-G. Suh, *et al.*, "Observation of the exceptional-point-enhanced Sagnac effect," Nature **576**, 65–69 (2019).
66. M. P. Hokmabadi, A. Schumer, D. N. Christodoulides, *et al.*, "Non-Hermitian ring laser gyroscopes with enhanced Sagnac sensitivity," Nature **576**, 70–74 (2019).
67. P.-Y. Chen, M. Sakhdari, M. Hajizadegan, *et al.*, "Generalized parity-time symmetry condition for enhanced sensor telemetry," Nat. Electron. **1**, 297–304 (2018).
68. C. M. Bender, B. K. Berntson, D. Parker, *et al.*, "Observation of PT phase transition in a simple mechanical system," Am. J. Phys. **81**, 173–179 (2013).
69. C. M. Bender, M. Gianfreda, Ş. K. Özdemir, *et al.*, "Twofold transition in PT-symmetric coupled oscillators," Phys. Rev. A **88**, 062111 (2013).
70. A. Regensburger, C. Bersch, M.-A. Miri, *et al.*, "Parity-time synthetic photonic lattices," Nature **488**, 167–171 (2012).
71. A. Guo, G. J. Salamo, and D. Duchesne, "Observation of PT-symmetry breaking in complex optical potentials," Phys. Rev. Lett. **103**, 093902 (2009).
72. H. Jing, Ş. K. Özdemir, X.-Y. Lü, *et al.*, "PT-symmetric phonon laser," Phys. Rev. Lett. **113**, 053604 (2014).
73. T. Kuang, R. Huang, W. Xiong, *et al.*, "Nonlinear multi-frequency phonon lasers with active levitated optomechanics," Nat. Phys. **19**, 414–419 (2023).
74. Z.-P. Liu, J. Zhang, Ş. K. Özdemir, *et al.*, "Metrology with PT-symmetric cavities: enhanced sensitivity near the PT-phase transition," Phys. Rev. Lett. **117**, 110802 (2016).
75. B. Peng, Ş. K. Özdemir, F. Lei, *et al.*, "Parity-time-symmetric whispering-gallery microcavities," Nat. Phys. **10**, 394–398 (2014).
76. L. Chang, X. Jiang, S. Hua, *et al.*, "Parity-time symmetry and variable optical isolation in active-passive-coupled microresonators," Nat. Photonics **8**, 524–529 (2014).
77. H. Jing, Ş. K. Özdemir, H. Lü, *et al.*, "High-order exceptional points in optomechanics," Sci. Rep. **7**, 3386 (2017).
78. Y.-L. Liu and Y.-X. Liu, "Energy-localization-enhanced ground-state cooling of mechanical resonator from room temperature in optomechanics using a gain cavity," Phys. Rev. A **96**, 023812 (2017).
79. G. S. Agarwal and K. Qu, "Spontaneous generation of photons in transmission of quantum fields in PT symmetric optical systems," Phys. Rev. A **85**, 031802 (2012).
80. K. V. Kepesidis, T. J. Milburn, J. Huber, *et al.*, "PT-symmetry breaking in the steady state of microscopic gain-loss systems," New J. Phys. **18**, 095003 (2016).
81. B. He, S. B. Yan, J. Wang, *et al.*, "Quantum noise effects with Kerr-nonlinearity enhancement in coupled gain-loss waveguides," Phys. Rev. A **91**, 053832 (2014).
82. B. He, L. Yang, Z. Zhang, *et al.*, "Cyclic permutation-time symmetric structure with coupled gain-loss microcavities," Phys. Rev. A **91**, 033830 (2015).
83. This claim will be discussed in Fig. 3.

84. C. Whittle, E. D. Hall, S. Dwyer, *et al.*, "Approaching the motional ground state of 10 Kg object," Science **372**, 1333–1336 (2021).
85. A. Kani, B. Sarma, and J. Twamley, "Intensive cavity-magnomechanical cooling of a levitated macromagnet," Phys. Rev. Lett. **128**, 013602 (2022).
86. D.-G. Lai, J.-F. Huang, X.-L. Yin, *et al.*, "Nonreciprocal ground-state cooling of multiple mechanical resonators," Phys. Rev. A **102**, 011502 (2020).
87. D.-G. Lai, F. Zou, B.-P. Hou, *et al.*, "Simultaneous cooling of coupled mechanical resonators in cavity optomechanics," Phys. Rev. A **98**, 023860 (2018).
88. D.-G. Lai, X. Wang, W. Qin, *et al.*, "Tunable optomechanically induced transparency by controlling the dark-mode effect," Phys. Rev. A **102**, 023707 (2020).
89. D.-G. Lai, J. Huang, B.-P. Hou, *et al.*, "Domino cooling of a coupled mechanical-resonator chain via cold-damping feedback," Phys. Rev. A **103**, 063509 (2021).
90. D.-G. Lai, W. Qin, B.-P. Hou, *et al.*, "Significant enhancement in refrigeration and entanglement in auxiliary-cavity-assisted optomechanical systems," Phys. Rev. A **104**, 043521 (2021).
91. D.-G. Lai, W. Qin, A. Miranowicz, *et al.*, "Efficient optomechanical refrigeration of two vibrations via an auxiliary feedback loop: giant enhancement in mechanical susceptibilities and net cooling rates," Phys. Rev. Res. **4**, 033102 (2022).
92. D.-G. Lai, Y.-H. Chen, W. Qin, *et al.*, "Tripartite optomechanical entanglement via opticaldark-mode control," Phys. Rev. Res. **4**, 033112 (2022).
93. See Supplement 1, which includes [94,95], for more details on: (i) our model Hamiltonian and the analysis of the exceptional point; (ii) the Langevin equations and their solutions; (iii) numerical and analytical results of the steady-state mean residual occupation numbers, effective susceptibilities, cooling rates, and noise spectra; and (iv) cooling performance of optomechanical networks.
94. E. X. DeJesus and C. Kaufman, "Routh-Hurwitz criterion in the examination of eigenvalues of a system of nonlinear ordinary differential equations," Phys. Rev. A **35**, 5288–5290 (1987).
95. I. S. Gradstein and I. M. Ryzhik, *Table of Integrals, Series, and Products*, 8th ed. (Academic, 2014).
96. A. Boltasseva and H. A. Atwater, "Low-loss plasmonic metamaterials," Science **331**, 290–291 (2011).
97. S. M. Kuo and D. R. Morgan, "Active noise control: a tutorial review," Proc. IEEE **87**, 943–975 (1999).